Journal of Molecular Structure 1028 (2012) 208–214

Contents lists available at SciVerse ScienceDirect

Journal of Molecular Structure

journal homepage: www.elsevier.com/locate/molstruc

Synthesis, structural characterization and anticancer activity of some new complexes of 6-amino-4-hydroxy-2-thiopyrimidine

Shadia A. Elsayed [a], Bertrand J. Jean-Claude [b], Ian S. Butler [c], Sahar I. Mostafa [d,*]

[a] Chemistry Department, Faculty of Science, Damietta, Mansoura University, Egypt
[b] Royal Victoria Hospital, Department of Medicine, Montreal, QC, Canada H3A 1A1
[c] Department of Chemistry, McGill University, Montreal, QC, Canada H3A 2K6
[d] Chemistry Department, Faculty of Science, Mansoura, Mansoura University, Egypt

ARTICLE INFO

Article history:
Received 10 March 2012
Received in revised form 28 May 2012
Accepted 29 May 2012
Available online 23 June 2012

Keywords:
Hahtp
Silver
Zinc
Palladium
Anticancer

ABSTRACT

New complexes of 6-amino-4-hydroxy-2-thiopyrimidine (Hahtp), $[Zn(ahtp)_2(H_2O)_2]$, $[Zn(ahtp)_2(PPh_3)(H_2O)]$, $[Zn(Hahtp)(bpy)Cl_2]$, [Pd(phen)(ahtp)]Cl, $[Pd(Hahtp)(PPh_3)_2]Cl_2$, $[Ag(ahtp)(H_2O)_2]$, $[Ag(ahtp)(PPh_3)(H_2O)]$, [Ag(ahtp)L] (L = bpy, phen), have been synthesized and characterized on the basis of spectral (IR, ^{1}H-NMR, ESI-mass and UV–visible), elemental analysis, thermal and molar conductivity measurements. Three modes of chelations have been observed for Hahtp; as a neutral bidentate ligand through cyclic nitrogen and thione sulfur atoms, mononegative bidentate ligand through either the deprotonated cyclic nitrogen and thione sulfur atoms or the deprotonated hydroxy and cyclic nitrogen atoms; all forming four-membered chelating rings. The free Hahtp and its complexes, $[Zn(ahtp)_2(H_2O)_2]$, $[Zn(Hahtp)_2(PPh_3)(H_2O)]$, $[Zn(Hahtp)(bpy)Cl_2]$, [Pd(phen)(Hahtp]Cl and $[Ag(Hahtp)(PPh_3)(H_2O)]$ have been tested against the human breast cancer MDA-MB231 cell line. The $[Ag(ahtp)(PPh_3)(H_2O)]$ complex exhibits the highest efficacy with a mean IC_{50} value of 4.7 μM.

1. Introduction

Pyrimidine constitutes are known as important component of nucleic acids and are reported as building blocks in pharmaceutics for the synthesis of antiviral, anticancer, antibacterial and antifungal agents [1–3]. Thus, the synthesis of new transition metal complexes with pyrimidine derivatives is a matter of interest because of their well known anti-cancer, anti-metastase and antimicrobial activity [4,5]. The pharmacological activity of these complexes comes from synergic effects by the transition metal ion and thiopyrimidine, once the coordinated molecule dissociates in the target tissue [6–8]. 2-Thiopyrimidine and 4,6-dimethyl-2-thiopyrimidine behave as unsymmetrical ambidentate ligands, when coordinate with metal ions, generate linkage isomerism due to steric-repulsion-interactions [9]. Palladium(II) thiopyrimidine complexes are of great interest due to the significant Pd(II)–S interactions in biological system [10]. During the past few years, our laboratory has been actively involved in the synthesis of a variety of complexes of 4,6-diamino-5-hydroxy-2-mercaptopyrimidine (Hdahmp) [11–13] and 5,6-diamino-2,4-dihydroxypyrimidine (Hahp) [14]. Some complexes of 4,6-diamino-5-hydroxy-2-mercaptopyrimidine have been evaluated for their antibacterial, antifungal [11,13] and anticancer activity [12]. Among them, the water soluble complexes, [Pd(bpy)(dahmp)]Cl and [Ag(bpy)(H-dahmp)]NO_3, display a significant anticancer activity against *Ehrlich ascites* tumor cells (EACs). In continuation of our search for potent active anticancer complexes, it was considered worthwhile to synthesize a variety of novel complexes of 6-amino-4-hydroxy-2-thiopyrimidine (Hahtp) with Zn(II), Pd(II) and Ag(I). The structures of the resulting complexes have been discussed on the bases of elemental analysis, spectral (IR, UV–visible, ^{1}H-NMR, mass), thermal and molar conductivity measurements. In addition, the anticancer activity of Hahtp and the complexes, $[Zn(ahtp)_2(H_2O)_2]$, $[Zn(Hahtp)(bpy)Cl_2]$, $[Zn(ahtp)_2(PPh_3)(H_2O)]$, [Pd(ahtp)(phen)]Cl, $[Pd(Hahtp)(PPh_3)_2]Cl_2$ and $[Ag(ahtp)(PPh_3)(H_2O)]$ have been tested against the human breast cancer MDA-MB231 cell line.

2. Experimental

2.1. Materials and measurements

All reagents and solvents were purchased from Alfa/Aesar and all manipulations were performed under aerobic conditions using materials and solvents as received. $[M(PPh_3)_2Cl_2]$ [15], $[M(bpy)Cl_2]$, $[M(phen)Cl_2]$ (M(II) = Pd, Pt) [16]. DMSO-d_6 was used for the NMR measurements referenced against TMS.

The human breast carcinoma MDA-MB-231 cell line was obtained from the American Type Culture Collection (ATCC catalog number). Cells were maintained in Dulbecco's Modified Eagle Med-

* Corresponding author. Tel.: +20 100 8502625; fax: +20 50 2246781.
E-mail address: sihmostafa@yahoo.com (S.I. Mostafa).

0022-2860/$ - see front matter © 2012 Elsevier B.V. All rights reserved.
http://dx.doi.org/10.1016/j.molstruc.2012.05.073

ium (Wisent Inc., St-Bruno, Canada) supplemented with 10% FBS, 10 mM HEPES, 2 mM L-gultamine and 100 μg/ml penicillin/streptomycin (GibcoBRL, Gaithersburg, MD). In all assays cells were plated 24 h before drug treatment.

Infrared spectra were recorded on a Nicolet 6700 Diamond ATR spectrometer in the 4000–200 cm^{-1} range. ^{1}H-NMR spectra were recorded on VNMRS 200 and 500 MHz spectrometer in DMSO-d_6 using TMS as reference. Mass spectra (ESI-MS) were recorded using LCQ Duo and double focusing MS25RFA instruments, respectively. Electronic spectra were recorded in DMF using a Hewlett–Packard 8453 spectrophotometer. Thermal analysis measurements were made in the 20–800 °C range at a heating rate of 20 °C min^{-1} using Ni and NiCo as references, on a on a TA instrument TGA model Q500Analyzer TGA-50. Molar conductivity measurements were carried out at room temperature on a YSI Model 32 conductivity bridge.

2.2. Preparations

2.2.1. $[Zn(ahtp)_2(H_2O)_2].2H_2O$

Zinc chloride (0.136 g, 1 mmol) in water (2 cm^3) was added to Hahtp (0.143 g, 1 mmol) in methanol containing KOH (0.056 g, 1 mmol; 15 cm^3). The reaction mixture was heated under reflux for 4 h, during which an off-white precipitate was obtained. This precipitate was filtered off, washed with water, methanol and air-dried. Yield: 81%. Anal. Calcd. for $C_{11}H_{22}N_6O_6S_2Zn$: C, 26.5; H, 4.4; N, 18.7; S, 14.3 %, Found: C, 26.9, H, 4.2; N, 17.9; S, 13.8%. Conductivity data (10^{-3} M in DMF): $\Lambda_M = 9.0\ \Omega^{-1}$. IR (cm^{-1}), 3320, 3416, 3318, 1621, 1521, 1377, 438, 332; ^{1}H NMR (d_6-DMSO/TMS, ppm), δ: 11.38 (s, 1H, O(4)H); 4.65 (s, 1H, C(5)H); 6.21 (s, 2H, NH_2), ESI-MS: *m/z*, 385.0 $[Zn(ahtp)_2(H_2O)_2]^+$, 349.5 $[Zn(ahtp)_2]^+$, 207.5$[Zn(ahtp)]^+$.

2.2.2. $[Zn(ahtp)_2(PPh_3)(H_2O)]$

$[ZnCl_2(PPh_3)_2]$ was prepared by refluxing a mixture of $ZnCl_2$ (0.136 g, 1 mmol) and triphenylphosphine (0.524 g, 2 mmol) in THF. Upon reducing the volume, white crystals were obtained.

$[Zn(PPh_3)_2Cl_2]$ (0.33 g, 0. 5 mmol) in dichloromethane (10 cm^3) was added to Hahtp (0.072 g, 0.5 mmol) in methanol (10 cm^3). The reaction mixture was heated under refluxed for 24 h and the white precipitate was filtered off, washed with methanol, dichloromethane and air-dried. Yield: 68%. Anal. Calcd.. for $C_{28}H_{29}N_6O_3PS_2Zn$: Calcd.: C, 51.1; H, 4.4; N, 12.7; S, 9.7%, Found: C, 50.6; H, 3.8; N, 12.1; S, 9.3%. Conductivity data (10^{-3} M in DMF): $\Lambda_M = 7.0\ \Omega^{-1}$. IR ($cm^{-1}$), 3538, 3432, 3323, 1595, 1505, 1381, 429, 326. ^{1}H NMR (d_6-DMSO/TMS, ppm), δ: 11.40 (s, 1H, O(4)H); 4.66 (s, 1H, C(5)H); 6.24 (s, 2H, NH_2).

2.2.3. $[Zn(Hahtp)(bpy)Cl_2]$

$ZnCl_2$ (0.068 g, 0.5 mmol) in water (2 cm^3) was added to basic methanolic solution {KOH (0.028 g, 0.5 mmol; 10 cm^3)} of Hahtp (0.072 g, 0.5 mmol). To the colorless solution, bpy (0.078 g, 0.5 mmol) in ethanol (10 cm^3) was added drop by drop with constant stirring. The reaction mixture was heated under reflux for 20 h. The white precipitate was filtered off, washed with methanol and air-dried. Yield: 76%. Anal. Calcd. for $C_{14}H_{13}Cl_2N_5OSZn$: C, 38.6; H, 3.0; N, 16.1; S, 7.3%, Found: C, 38.3; H, 2.6; N, 16.3; S, 6.8%. Conductivity data (10^{-3} M in DMF): $\Lambda_M = 8.0\ \Omega^{-1}$. IR ($cm^{-1}$), 3331, 3412, 3329, 1626, 1523, 1377, 439, 341. ^{1}H NMR (d_6-DMSO/TMS, ppm), δ: 11.42 (s, 1H, N(1)H); 11.35 (s, 1H, O(4)H); 4.70 (s, 1H, C(5)H); 6.37 (s, 2H, NH_2). ESI-MS (*m/z*): 436.0 $[Zn(Hahtp)(bpy)Cl_2]^+$, 363.0 $[Zn(bpy)]^+$.

2.2.4. $[Pd(phen)(ahtp]Cl$

$[Pd(phen)Cl_2]$ (0.085 g, 0.25 mmol) in methanol–benzene (3:2 V/V, 5 cm^3) was added to Hahtp (0.036 g, 0.25 mmol) in methanol containing KOH (0.014 g, 0.25 mmol; 10 cm^3). The reaction mixture was stirred with warming for 96 h. The yellow precipitate was filtered off, washed with methanol and air-dried. Yield: 64%. Anal. Calcd. for $C_{16}H_{12}ClN_5OPdS$: C, 43.9; H, 3.3; N, 14.1; S, 6.5%, Found: C, 43.6; H, 3.2; N, 14.0; S, 6.3%. Conductivity data (10^{-3} M in DMF): $\Lambda_M = 96.0\ \Omega^{-1}$. IR ($cm^{-1}$): 3423, 3316, 2953, 1613, 1541, 1373, 500, 432. ^{1}H NMR (d_6-DMSO/TMS, ppm), δ: 11.22 (s, 1H, N(1)H); 4.56 (s, 1H, C(5)H); 5.66 (s, 2H, NH_2). ESI-MS (*m/z*): 430 $[Pd(ahtp)(phen)]^+$, 285 $[Pd(phen)]^+$.

2.2.5. $[Pd(Hahtp)(PPh_3)_2Cl_2]$

$[Pd(PPh_3)_2Cl_2]$ (0.14 g, 0.2 mmol) was added to Hahtp (0.03 g, 0.2 mmol) in dichloromethane (10 cm^3). The mixture was heated under reflux for 48 h. The green-yellow precipitate was filtered off, washed with dichlromethane and air-dried. Yield: 59%. Anal. Calcd. for $C_{40}H_{35}Cl_2N_3OP_2PdS$: C, 56.8; H, 4.1; N, 4.9; S, 3.8%, Found: C, 56.1; H, 3.8; N, 4.3; S, 3.7%. Conductivity data (10^{-3} M in DMF): $\Lambda_M = 98.0\ \Omega^{-1}$. IR ($cm^{-1}$): 3334, 3425, 3316, 2960, 1606, 1504, 1378, 442, 333. ^{1}H NMR (d_6-DMSO/TMS, ppm), δ: 11.22 (s, 1H, N(1)H) ; 11.59 (s, 1H, O(4)H); 4.65 (s, 1H, C(5)H); 6.35 (s, 2H, NH_2). ESI-MS (*m/z*): 774 $[Pd(Hahtp)(PPh_3)_2]^+$, 511.0 $[Pd(PPh_3)(Hahtp)]^+$.

2.2.6. $[Ag(ahtp)(H_2O)_2].H_2O$

Silver nitrate (0.17 g, 1 mmol) in water (2 cm^3) was added to Hahtp (0.143 g, 1 mmol) in methanol containing KOH (0.056 g, 1 mmol; 10 cm^3). The reaction mixture was heated with stirring for 4 h in the dark and the white precipitate was filtered off, washed with water, methanol and air-dried in dark. Yield: 81%. Anal. Calcd. for $C_4H_8AgN_3O_3S$: C, 15.7; H, 3.2; N, 13.7; S, 10.6%, Found: C, 15.2, H, 3.0 N, 13.4; S, 10.5%. Conductivity data (10^{-3} M in DMF): $\Lambda_M = 9.0\ \Omega^{-1}$. IR ($cm^{-1}$): 3322, 3426, 3317, 1623, 1548, 1396, 437, 331. ^{1}H NMR (d_6-DMSO/TMS, ppm), δ: 12.08 (s, 1H, O(4)H), 4.84 (s, 1H, C(5)H) ; 6.61 (s, 2H, NH_2). ESI-MS (*m/z*): 290.0 $[Ag(ahtp)(H_2O)_2]^+$, 167.0 $[Ag(ahtp\text{-}C_3H_4N_2O)]^+$.

2.2.7. $[Ag(ahtp)(PPh_3)(H_2O)]$

In the dark, silver nitrate (0.087 g, 0.5 mmol) in water (2 cm^3) was added to PPh_3 (0.131 g, 0.5 mmol) in methanol (15 cm^3) and the colorless solution was stirred for 3 h. This solution was added to Hahtp (0.07 g, 0.5 mmol) in methanol containing KOH (0.028 g, 0.5 mmol; 10 cm^3). The reaction was stirred for 48 h. The white solid was filtered off, washed with water, methanol and air-dried. Yield: 79%. Anal. Calcd. for $C_{22}H_{21}AgN_3O_2PS$: C, 49.8; H, 3.9; N, 7.9; S, 6.0%. Found: C, 49.2; H, 4.1; N, 8.5; S, 5.4%. Conductivity data (10^{-3} M in DMF): $\Lambda_M = 8.0\ \Omega^{-1}$. IR ($cm^{-1}$): 3343, 3429, 3344, 1638, 1512, 1360, 444,329. ^{1}H NMR (d_6-DMSO/TMS, ppm), δ: 11.25 (s, 1H, O(4)H); 4.69 (s, 1H, C(5)H), 6.25 (s, 2H, NH_2). ESI-MS (*m/z*): 535 $[Ag(PPh_3)(ahtp)(H_2O)]^+$, 371.0 $[Ag(PPh_3)]^+$.

2.2.8. $[Ag(ahtp)L]$ (L = bpy, phen)

A similar procedure as for the $[Ag(PPh_3)(Hahtp)(H_2O)]$ analogue was applied using bpy (0.078 g, 0.5 mmol) or phen (0.09 g, 0.5 mmol) instead of PPh_3. The white (bpy) or yellow (phen) precipitate was filtered off, washed with water, methanol and air-dried.

2.2.8.1. For [Ag(bpy)(ahtp)]. Yield: 80%. Anal. Calcd. for $C_{14}H_{12}AgN_5OS$: C, 41.4; H, 2.9; N, 17.2; S, 7.8%, Found: C, 41.1; H, 2.2; N, 17.2, S, 7.3%.Conductivity data (10^{-3} M in DMF): $\Lambda_M = 6.0\ \Omega^{-1}$. IR ($cm^{-1}$): 3314, 3430, 3320, 1622, 1517, 1380, 436, 332. ^{1}H NMR (d_6-DMSO/TMS, ppm), δ: 11.83 (s, 1H, O(4)H), 4.81 (s, 1H, C(5)H), 6.65 (s, 2H, NH_2). ESI-MS (*m/z*): 405 $[Ag(bpy)(ahtp)]^+$.

2.2.8.2. For [Ag(phen)(ahtp)]. Yield: 78%. Anal. Calcd. for $C_{16}H_{12}AgN_5OS$: C, 44.4; H, 3.3; N, 16.3; S, 7.4%. Found: C, 44.0; H, 3.2; N, 15.8; S, 7.0%. Conductivity data (10^{-3} M in DMF): $\Lambda_M = 6.0\ \Omega^{-1}$. IR ($cm^{-1}$): 3321, 3422, 3328, 1646, 1510, 1392, 457, 342. ^1H NMR (d_6-DMSO/TMS, ppm), δ: 12.14 (s, 1H, O(4)H), 4.85 (s, 1H, C(5)H), 6.59 (s, 2H, NH_2). ESI-MS (*m/z*): 431 $[Ag(phen)(ahtp)]^+$.

2.3. Biological assay

Growth inhibition assay; MDA-MB-231 cells were plated at 2500 cells/well in 96-well flat-bottomed microliter plates (Costar, Corning, NY). After 24 h incubation, the cells were exposed to different concentrations of each compound continuously for 5 days. Briefly, following drug treatment, the cells were fixed using 50 μl of cold trichloroacetic acid (50%) for 2 h at 4 °C, washed with water, stained with sulforhodamine B (SRB 0.4%) overnight at room temperature, rinsed with 1% acetic acid and allowed to dry overnight [17]. The resulting colored residue was dissolved in 200 μl Tris base (10 mM, pH 10.0) and optical density was recorded at 490 nm using a microplate reader ELx808 (BioTek Instruments). The results were analyzed by GraphPad Prism (GraphPad Software, Inc., San Diego, CA) and the sigmoidal dose response curve was used to determine 50% cell growth inhibitory concentration (IC_{50}). Each point represents the average of two independent experiments performed in triplicate [17].

3. Results and discussion

The experimental section describes the synthesis of some new complexes of 6-amino-4-hydroxy-2-thiopyrimidine (Hahtp). The elemental analyses of the complexes are in excellent agreement with the assigned formulae. The molar conductivities (Λ_M) in DMF at room temperature suggest all complexes to be non-electrolytes except for, [Pd(ahtp)(phen)]Cl and $[Pd(Hahtp)(PPh_3)_2]Cl_2$, which show 1:1 and 1:2 electrolytes, respectively [12,18]. The complex, $[Zn(ahtp)_2(H_2O)_2]$ was prepared from Hahtp and $ZnCl_2$ in methanol under basic conditions. $[Zn(ahtp)_2(PPh_3)(H_2O)]$ and $[Pd(Hahtp)(PPh_3)]Cl_2$ were isolated from the reaction of $[M(PPh_3)_2Cl_2]$ (M(II) = Zn, Pd) and Hahtp in CH_2Cl_2 under reflux. The complex, $[Zn(Hahtp)(bpy)Cl_2]$, was prepared from $ZnCl_2$, Hahtp and 2,2′-bipyridyl under basic conditions. The reaction of Hahtp and $[Pd(phen)Cl_2]$ in basic methanol–benzene produced [Pd(phen)(ahtp)]Cl. The complex, $[Ag(ahtp)(H_2O)_2]$, was isolated from the reaction of Hahtp and $AgNO_3$ in basic methanol in the dark while the complexes, $[Ag(ahtp)(PPh_3)(H_2O)]$ and [Ag(ahtp)L] (L = bpy, phen) were formed from the reaction of $AgNO_3$ with Hahtp in presence of PPh_3, bpy or phen in methanol under basic conditions in the dark.

3.1. Vibrational spectra

The characteristic IR bands and vibrational assignments observed for 6-amino-4-hydroxy-2-thiopyrimidine (Hahtp) complexes are reported in the experimental section. The IR spectral data of Hahtp support its existence in the thione form (Scheme 1). This conclusion is supported by the presence of the ν(NH) stretch at 2950 cm^{-1} [19], the absence of the ν(SH) mode near 2600 cm^{-1}, and the production of the characteristic thioamide bands due to extensive coupling of δ(NH), ν(C=N), ν(NCS), and ν(C=S) at 1623, 1585, and (1375, 1268, 1179) cm^{-1}, respectively [20–22]. The bands at 3422 and 3317 cm^{-1} are due to $\nu_{as}(NH_2)$ and $\nu_s(NH_2)$ stretching vibration, respectively, while the strong band at 3315 cm^{-1} is associated with the ν(OH) stretching vibration [12,14,23].

In the complexes, $[Zn(ahtp)_2(H_2O)_2]$, $[Zn(ahtp)_2(PPh_3)(H_2O)]$, $[Ag(ahtp)(H_2O)_2]$, $[Ag(ahtp)(PPh_3)(H_2O)]$, [Ag(ahtp)L] (L = bpy, phen), Hahtp acts as a mononegative bidentate ligand, coordinating the metal ions through the thione sulfur and the deprotonated cyclic nitrogen N(1) atoms [9,12,14]. This feature is evidenced by the shift observed in the ν(C=S) and ν(N—C=S) stretching modes as well as the absence of the ν(NH) and δ(NH) stretches [12,14]. Moreover, the existence of $\nu_s(NH_2)$, $\nu_{as}(NH_2)$, and ν(OH) stretches more or less in the same position as in the free ligand [20,24,25]. These results indicate the replacement of the acidic hydrogen by the metal ion, forming four-membered chelate ring [9]. The same feature have been observed and support by X-ray crystal structures of $[Pd_2(Tu)(PPh_3)_3Cl_2]$ and *trans–cis–cis*-$[Ru(AsPh_3)_2(Tpy)]$ (Tu = 2-thiouracil, Tpy = 2-thiopyrimidine) complexes [9,20]. Figs. 1 and 2 show the structures of $[Zn(ahtp)_2(H_2O)_2]$ and [Ag(ahtp)(bpy)], respectively.

In the [Pd(ahtp)(phen)]Cl complex (Fig. 3), the ν(OH) stretching vibration at 3315 cm^{-1} in the free ligand is missing, while the bands arising from ν(C=N) are shifted to lower wavenumber [26,27]. The bands arising from the $\nu_{as}(NH_2)$, $\nu_s(NH_2)$, ν(NH), δ(NH), ν(NCS) and ν(C=S) modes are not affected by complexation. This feature supports the coordination of $ahtp^-$ through the deprotonated hydroxy oxygen and cyclic nitrogen N(3) centers without any participation of the thione sulfur atom due to the observation of a band near 1178 cm^{-1} ariseing from the ν(C=S) stretch that remains unchanged [11,13,14].

The IR spectra of the $[Zn(bpy)(Hahtp)Cl_2]$ and $[Pd(Hahtp)(PPh_3)_2]Cl_2$ complexes (Fig. 4) show that Hahtp functions as a neutral bidentate ligand coordinating Zn(II) or Pd(II) through the thione sulfur and cyclic nitrogen N(3) atoms. This mode of chelation is evidenced by the shifts observed for ν(C=N), ν(C=S) and ν(N—C=S) stretches, while the bands arising from ν(OH), $\nu_{as}(NH_2)$, $\nu_s(NH_2)$, ν(NH) and δ(NH) are found more or less in the same positions as in the free ligand [12].

As expected, the presence of coordinated PPh_3 in the complexes $[Zn(ahtp)_2(PPh_3)(H_2O)]$, $[Pd(Hahtp)(PPh_3)_2]Cl_2$ and $[Ag(ahtp)(PPh_3)(H_2O)]$ is indicated by strong IR bands near 1100 and 750 cm^{-1} due to ν(P—C) and δ(CCH) vibrations, respectively [13,28]. Also, the IR bands near 1590, 1510, 1480 and 1423 cm^{-1} in the complexes, [Pd(ahtp)(phen)]Cl and [Ag(ahtp)(phen)], are due to the phen stretching vibrations [29]. These bands are at high-

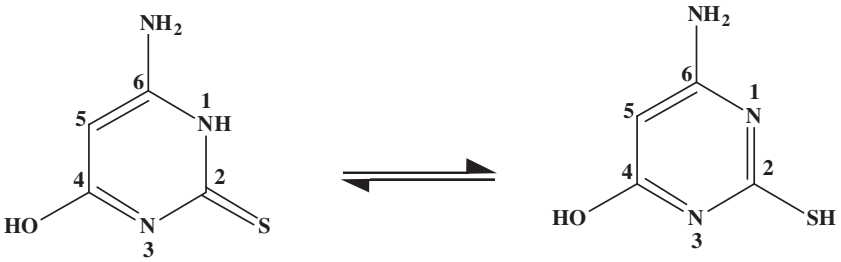

Scheme 1. Thione-thiol form of 6-amino-4-hydroxy-2-thiopyrimidine (Hahtp).

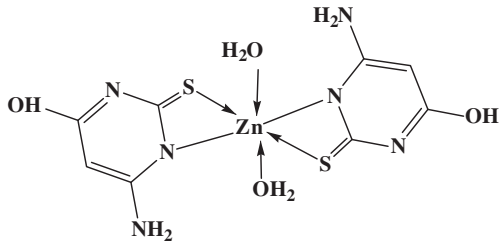

Fig. 1. Structure of $[Zn(ahtp)_2(H_2O_2)_2]$.

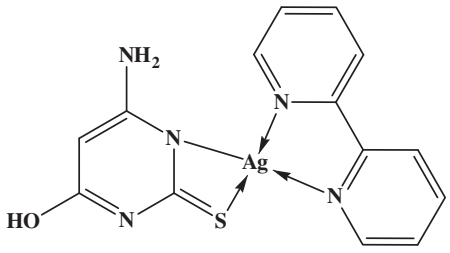

Fig. 2. Structure of [Ag(ahtp)(bpy)].

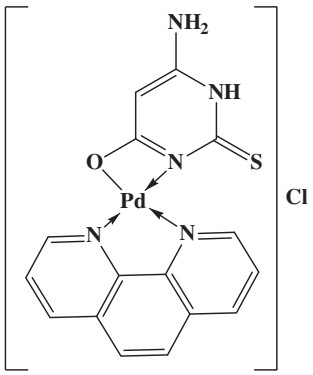

Fig. 3. Structure of [Pd(Hahtp)(phen)]Cl.

er wavenumbers compared with those for the free phen ligand indicating chelation. Also, in the complexes, $[Zn(Hahtp)(bpy)Cl_2]$ and [Ag(ahtp)(bpy)], the bands near 840, 750 and 725 cm^{-1} are assigned to coordinated bpy [30].

The spectra of the complexes show several bands near 500, 420, 350 and 290 cm^{-1} due to ν(M—O), ν(M—N), ν(M—S) and ν(M—Cl) stretches, respectively [13,31]. In the complex $[Zn(Hahtp)(bpy)Cl_2]$, one sharp band is observed at 300 cm^{-1}, corresponding to the presence of the *trans*-$ZnCl_2$ moiety [11,32].

3.2. NMR spectra

The ^{1}H-NMR data for the free Hahtp ligand and some of its complexes in DMSO-d_6 are given in the experimental section. The ^{1}H-NMR spectrum of Hahtp shows four singlets at δ 4.67, 6.35, 11.51 and 11.60 ppm arising from H(5), NH_2(6), NH(1) and OH(4), respectively (see Fig. 5 for numbering scheme).

In the ^{1}H NMR spectra of the complexes, $[Zn(ahtp)_2(PPh_3)(H_2O)]$, $[Zn(ahtp)_2(H_2O)_2]$, $[Ag(ahtp)(H_2O)_2]$, $[Ag(ahtp)(PPh_3)(H_2O)]$ and [Ag(ahtp)L] (L = bpy, phen), the NH(1) singlet is not observed, while that of NH_2 appears upfield confirming the coordination of $ahtp^-$ through the thione sulfur and deprotonated cyclic N(1) atoms [9,12,14,33].

In the spectrum of the complex, [Pd(ahtp)(phen)]Cl, the hydroxy proton, OH(4), signal is not observed while the H(5) signal is

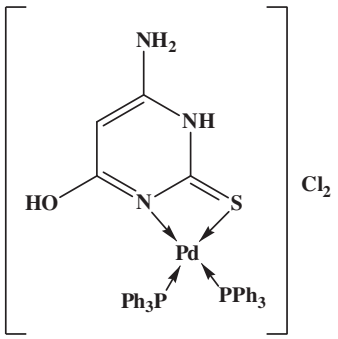

Fig. 4. Structure of $[Pd(Hahtp)](PPh_3)_2]Cl_2$.

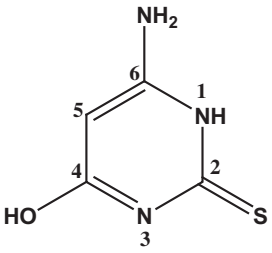

Fig. 5. Structure of 6-amino-4-hydroxy-2-thiopyrimidine (Hahtp).

shifted upfield. This feature supports coordination of $ahtp^-$ through the deprotonated hydroxy and cyclic nitrogen N(3) atoms [11–14].

In spectra of the complexes, $[Zn(Hahtp)(bpy)Cl_2]$ and $[Pd(Hahtp)(PPh_3)_2]Cl_2$, the four singlets are observed with upfield shifts for the OH(4) and NH(1) protons indicating the coordination of Hahtp to Zn(II) or Pd(II) through the thione and cyclic nitrogen N(3) atoms [12,20]. The signals for H(5) and H(6) are shifted upfield, which may be attributed to the decrease in the electron density in the pyrimidine ring upon complexation [34].

3.3. Electronic spectra

The electronic spectra of the complexes were recorded in DMSO in the 200–800 nm range. The electronic spectra of the diamagnetic silver(I) complexes, $[Ag(ahtp)(H_2O)_2]$, $[Ag(PPh_3)(ahtp)]$ and [Ag(ahtp)L] (L = bpy, phen), show bands near 445 and 380 nm; the latter may arise from charge transfer of the type ligand(π) → b_{1g} (Ag^+) and ligand (σ) → b_{1g} (Ag^+), respectively, in distorted square planar environment around the metal ion [35].

The electronic spectra of the diamagnetic [Pd(phen)(ahtp)]Cl and $[Pd(PPh_3)_2(ahtp)]Cl_2$ complexes show bands near 475 and 330 nm due to $^1A_{1g} \rightarrow {}^1B_{1g}$ and $^1A_{1g} \rightarrow {}^1E_{1g}$ transitions in a square-planar configuration [12,34,36]. The absorption band near 375 nm is assigned to combination of charge-transfer transitions from the Pd(II) d-orbital to the π^*-orbital of phen or PPh_3 [37].

3.4. Mass spectra

The mass spectra of the complexes, $[Zn(ahtp)_2(H_2O)_2]$, $[Zn(Hahtp)(bpy)Cl_2]$, [Pd(phen)(ahtp)]Cl, $[Pd(PPh_3)_2(Hahtp)]Cl_2$, [AgL(ahtp)] (L = bpy, phen), $[Ag(ahtp)(H_2O)_2]$ and $[Ag(ahtp)(PPh_3)(H_2O)]$, are reported in the experimental section and their molecular ion peaks are in agreement with their assigned formulae. The mass spectrum of $[Zn(ahtp)_2(H_2O)_2]$ shows fragmentation patterns corresponding to the successive degradation of the complex. The first peak at *m/z* 385.0 with 6% abundance represents the molecu-

Table 1
Anticancer activity of 6-amino-4-hydroxy-2-thiopyrimidine and its complexes against human breast cancer MDA-MB-231 cell line.

Compound	IC_{50} (μM)
Hahtp	>100
[Zn(bpy)(Hahtp)Cl_2]	>100
[Zn(ahtp)$_2$(PPh_3)(H_2O)]	49.6
[Zn(ahtp)$_2$(H_2O)$_2$]	>100
[Pd(phen)(ahtp)]Cl	7.7
[Pd(Hahtp)(PPh_3)$_2$]Cl_2	24.5
[Ag(ahtp)(PPh_3)(H_2O)]	4.7
Cis-platin	8.7

lar ion (Calcd. 385.5). The peaks at 349.5 and 207.5 correspond to $[Zn(ahtp)_2]^+$ and $[Zn(ahtp)]^+$ fragments, respectively. The mass spectrum of [Zn(Hahtp)(bpy)Cl_2] shows a peak at *m/z* 436.0 (Calcd. 435.5), in agreement with the molecular ion of the complex, $[Zn(Hahtp)(bpy)Cl_2]^+$, with 3.2% abundance. There are signals which represent the loss of Cl_2 and $C_3H_4N_2O$ fragments (Calcd. 364.5) and $[Zn(bpy)]^+$ with *m/z* 221 (Calcd. 221.5), respectively. The mass spectrum of [Pd(phen)(ahtp)]Cl displays a signal at *m/z* 430 (Calcd. 328.4) with 100% abundance, in agreement with the molecular ion of the complex, $[Pd(ahtp)(phen)]^+$. The fragmentation patterns indicate ahtp loss to $[Pd(phen)]^+$ at 285 (Calcd. 286.4). The mass spectrum of the [Pd(PPh_3)$_2$(Hahtp)]Cl_2 complex shows first the molecular ion peak at *m/z* 774 (Calcd. 773.4) with 35% abundance, in agreement with the molecular ion, $[Pd(Hahtp)(PPh_3)_2]^+$. The fragmentation patterns indicate the loss of PPh_3, $[Pd(PPh_3)(Hahtp)]^+$ at 511 (Calcd. 511.4), [16,38]. The mass spectrum of [Ag(ahtp)(H_2O)$_2$] shows signal at *m/z* 290 (Calcd. 286) represents the molecular peak of the complex, $[Ag(ahtp)(H_2O)_2]^+$. The spectrum exhibits one more peak at 167 (Calcd. 166) corresponding $[Ag(ahtp\text{-}C_3H_4N_2O)]^+$ [14]. The mass spectrum of [Ag(P-Ph_3)(ahtp)(H_2O)] exhibits the first signal at *m/z* 535 (Calcd. 530) corresponding to $[Ag(ahtp)(PPh_3)(H_2O)]^+$ while the second one at 371 (Calcd. 370) corresponding to $[Ag(PPh_3)]^+$ fragment [12,14].

The mass spectra of [Ag (ahtp)L] (L = bpy, phen) show peaks at *m/z* 405 and 431 (Calcd. 406 and 430) with 5% and 10% abundance, respectively.

3.5. Thermal measurements

The thermal stability and degradation behavior of some reported complexes, [Zn(Hahtp)(bpy)Cl_2], [Zn(ahtp)$_2$(PPh_3)(H_2O)], [Pd(phen)(ahtp)]Cl.2H_2O, [Pd(PPh_3)$_2$(Hahtp)]Cl_2 and [Ag(P-Ph_3)(ahtp)(H_2O)] were studied using the thermogravimetric (TG) technique. The weight loss observed below 130 °C is due to dehydration as the colors changed from pale to deeper [33,39].

The thermogram of [Pd(PPh_3)$_2$(Hahtp)]Cl_2, shows four TG inflections in the 35–210, 211–270, 271–520 and 525–800 °C regions. These weight losses may arise from the release of chlorine molecule (Calcd. 8.4, Found 8.3), three Ph (Calcd. 27.4, Found 27.2%), two P, three Ph and N_2 fragments (Calcd. 38.0, Found 38.3%), and C_4H_5S (Calcd. 10.1, Found 9.5%) fragments, respectively [33], leaving a residue of palladium oxide and nitride (18.1%). The thermogram of [Zn(Hahtp)(bpy)Cl_2], is characterized by four weight losses in the 50–300, 301–420, 421–500 and 501–800 °C regions. These weight losses are due to the elimination of Cl_2 (Calcd. 16.3, Found 16.1%) [12], $C_3H_5N_2$ (Calcd. 15.8, Found 15.4%), CNS (Calcd. 13.3, Found 13.2%) and 1/2 bpy (Calcd. 17.9, Found 18.2%) fragments, respectively, leaving ZnO contaminated

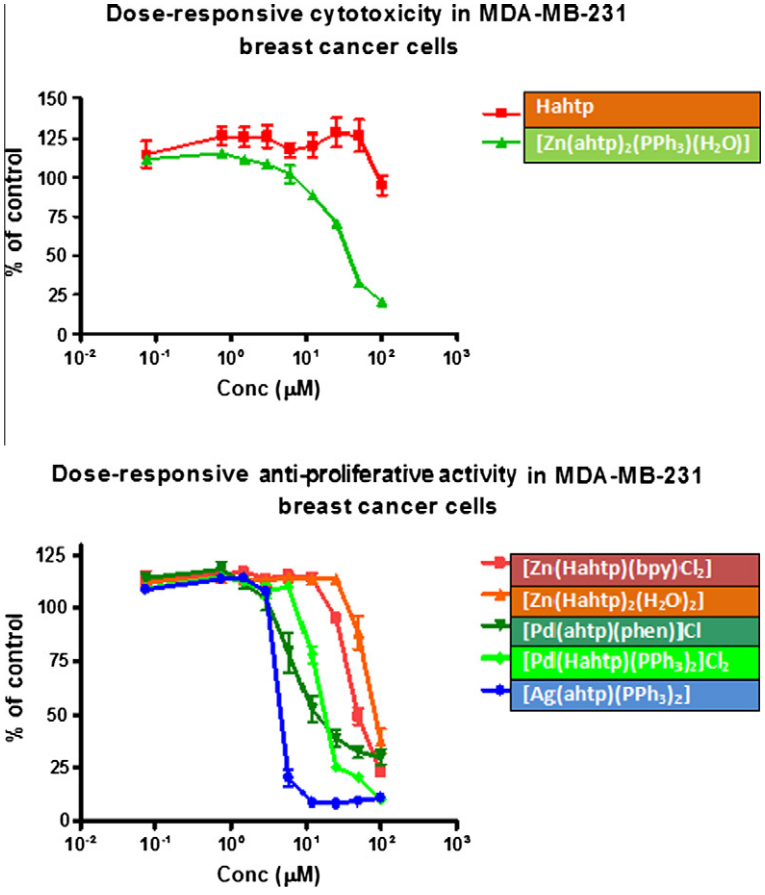

Fig. 6. Anticancer activity of of Hahtp and its complexes against the human breast cancer MDA- MB231 cell line.

with carbide residue at 700 °C (31.7%) [12,33]. The TG thermogram of [Pd(phen)(ahtp)]Cl.2H_2O shows the first endothermic weight loss step between 25 and 265 °C, corresponding to the release of crystal lattice water and 1/2Cl_2 (Cacld. 14.3, Found 14.8%). The second decomposition step occurs between 266 and 430 °C, this weight loss is attributed the loss of $C_4H_3N_2S$ fragment (Calcd. 22.2, Found 22.3%). The third TG inflection between 431 and 800 °C is attributed to the loss of C_6H_2 and 1/2N_2 fragments (Calcd. 17.6, Found 17.0%), leaving PdO and carbide residue representing (45.9%). In some reported transition metal complexes, the thermal decomposition residue is mainly metal or metal oxide, but in the presence of non-stoichiometric oxide, unburned carbon or nitrogen is observed [23].

The thermal decomposition of the complex [Zn(ahtp)$_2$(PPh_3)(-H_2O)], shows two TG inflections in the ranges of 75–326 and 327–800 °C. The exothermic weight losses may arise from the release of coordinated water, PPh_3, 1/2O_2 and two $C_4H_4N_3S$ fragments (Calcd. 87.1, Found 86.9%), and zinc oxide residue (Calcd. 13.1, Found 12.9%), respectively [33].

The TG thermogram of the complex [Ag(ahtp)(PPh_3)(H_2O)], displays three TG weight losses in the ranges 200–275 °C, 276–345 and 346–800 °C. The first exothermic weight loss may arise from the release of coordinated water, three Ph and 1/2N_2 fragments (Calcd. 49.6, Found 50.2%). The second one is due to the loss of one P (Calcd. 5.8, Found 5.7%) while the third is indicating the loss of $C_4H_4O_{1/2}S$ fragment (Calcd. 17.4, Found 17.2%), leaving silver oxide residue (26.9%) [12].

3.6. Anti-cancer activity

Cisplatin is perhaps the best known example of small molecule metal-containing drug, which acts as an anticancer agent in several human cancers, particularly, testicular and ovarian cancers [12,40]. Side effects, especially nephrotoxicity, of this drug limit its widespread use in high doses [41]. The need to develop new complexes with reduced nephrotoxicity and higher activity has stimulated the synthesis of many new complexes. Over the past years, a renewed interest in Pd(II) and Ag(I) complexes as potential anticancer agents has developed [12,23,33,34,42]. Though a number of interesting Pd(II) targets have been investigated [12,23,33,42], the biological utility of such agents continues to be questioned; this may be due to the poor solubility of these complexes under physiological conditions. Many 2-mercaptopyrimidine and 2-mercapto-4-aminopyrimidine are able to inhibit the synthesis of *t*-RNA, and thus, they may act as valuable substrates in the synthesis of promising antitumor chemotherapeutic agents [43].

The goal of this study was to develop 2-thiopyrimidine mixed ligand complexes containing nitrogen bases with high efficacy against cancer cells. The in vitro cytotoxicity of the free Hahtp and its complexes; [Zn(ahtp)$_2$(H_2O)$_2$], [Zn(Hahtp)(bpy)Cl_2], [Zn(ahtp)$_2$(PPh_3)(H_2O)], [Pd(ahtp)(phen)]Cl, [Pd(Hahtp)(PPh_3)$_2$]Cl_2 and [Ag(ahtp)(PPh_3)(H_2O)] were examined against the human breast cancer MDA-MB231 cell line in comparison with cis-platin as a reference, and the results are given in Table 1 and Fig. 6. Both [Pd(phen)(ahtp)]Cl and [Ag(PPh_3)(ahtp)(H_2O)] complexes exhibit remarkable growth inhibitory activities with mean IC_{50} values of 7.7 and 4.7 μM, respectively; cis-platin, IC_{50} value is 8.7 μM. The complexes, [Pd(phen)(ahtp)]Cl and [Ag(PPh_3)(ahtp)(H_2O)] show greater efficiency than do Hahtp, [Zn(ahtp)$_2$(H_2O)$_2$], [Zn(Hahtp)(bpy)Cl_2], [Zn(ahtp)$_2$(PPh_3)(H_2O)] and [Pd(Hahtp)(PPh_3)$_2$]Cl_2; this observation may be due to the structure–activity rules, the mode of chelation of $ahtp^-$ as well as the activity of the second ligand (phen or PPh_3) [33,42]. It has been reported that [Pt(R-phen)Cl_2] (R-phen = variety of substituted 1,10-phenanthrolines) act as agents capable of intercalating into the DNA double helix rather than forming coordinating covalent adducts [44]. This indicate that, the water soluble complex, [Pd(phen)(ahtp)]Cl may able to reach DNA as a cellular target, which can be determined by intracellular transport factors [45]. On the other side, the highest efficacy of the silver complex, [Ag(ahtp)(PPh_3)(H_2O)], is expected, since Ag(I) has been reported as a wound healing stimulator [46–48].

4. Conclusions

In conclusion, new complexes of Hahtp have been prepared and characterized. The Hahtp ligand shows different coordination modes-mononegative bidentate, through either thione sulfur and deprotonated cyclic nitrogen N(1) centers or deprotonated hydroxy oxygen and cyclic nitrogen N(3) centers, and neutral bidentate thione sulfur and cyclic nitrogen N(3) centers. The free hahtp ligand and its complexes, [Zn(bpy)(Hahtp)Cl_2], [Zn(ahtp)$_2$(PPh_3)(H_2O)], [Zn(ahtp)$_2$(H_2O)$_2$], [Pd(phen)(ahtp)]Cl, [Pd(Hahtp)-(PPh_3)$_2$]Cl_2 and [Ag(ahtp)(PPh_3)(H_2O)], have been tested as anticancer agents against MDA-MB231 breast cancer cells and the silver(I) complex, [Ag(ahtp)(PPh_3)(H_2O)], shows high efficacy.

Acknowledgements

We are grateful to the Ministry of Higher Education in Egypt (ES) and NSERC (Canada) Discovery Grant (ISB) for the financial support of this work.

References

[1] K.K. Ogilvie, R.G. Hamilton, M.F. Gillen, B.K. Radatus, K.O. Smith, K.S. Galloway, Can. J. Chem. 62 (1984) 16.
[2] N. Zenker, Thyroid function and thyroid drugs, in: W.O. Foye (Ed.), Principles of Medicinal Chemistry, third ed., Lea & Febiger, Philadelphia, London, 1990, p. 603.
[3] M.B. Deshmukh, S.M. Salunkhe, D.R. Patil, P.V. Anbhule, Eur. J. Med. Chem. 44 (2009) 2651.
[4] B. Lippert, Alteration of nucleobase p*K*a values upon metal coordination; origin and consequences, in: K.D. Karlin (Ed.), Prog. Inorg. Chem., vol. 54, 2005 (Chapter 6).
[5] K. Karidi, A. Garoufis, N. Hadjiliadis, M. Lutz, A. Spek, J. Reedijk, Inorg. Chem. 45 (2006) 10282.
[6] A. Dobrov, V.B. Arion, N. Kandler, W. Ginzinger, M.A. Jakupec, A. Rufinska, N. Graf von Keyserlingk, M. Galanski, C. Kowol, B.K. Keppler, Inorg. Chem. 45 (2006) 1945.
[7] T.M. Hunter, I.W. McNae, X. Liang, J. Bella, S. Parsons, M.D. Walkinshaw, P.J. Sadler, Nat. Acad. Sci. USA 102 (2005) 2288.
[8] R.A. Alderden, H.R. Mellor, S. Modok, T.W. Hambley, R. Callaghan, Biochem. Pharmacol. 71 (2006) 1136.
[9] F. Shaheen, A. Badashah, M. Gielen, L. Marchio, D. deVos, M.K. Khosa, Appl. Organomet. Chem. 21 (2007) 626.
[10] V. Montoya, J. Pons, X. Solans, M. Font-bardia, J. Ros, Inorg. Chim. Acta 358 (2005) 2312.
[11] S.I. Mostafa, N. Hadjiliadis, Transition Met. Chem. 33 (2008) 529.
[12] S.I. Mostafa, F.A. Badria, Metal-Based, Drugs, doi: 10.1155/2008/723634.
[13] S.I. Mostafa, C. Papatriantafyllopoulou, S. Perlepes, N. Hadjiliadis, Bioinorg. Chem. Appl., doi:10.1155/2008/647873.
[14] S.I. Mostafa, M.A. Kabil, E.M. Saad, A.A. El-Asmy, J. Coord. Chem. 59 (2006) 279.
[15] R.C. Cookson, D.W. Jones, J. Chem. Soc. (1965) 1881.
[16] W.P. Griffith, S.I. Mostafa, Polyhedron 11 (1992) 871.
[17] P. Skehan, R. Storeng, D. Scudiero, J. Natl Cancer Inst. 82 (1990) 1107.
[18] M.A. Romero, M.P. Sànchez, M. Quiròs, F. Sànchez, J.M. Salas, M.N. Moreno, R. Faure, Canada J. Chem. 71 (1993) 29.
[19] Z. Popovic, D.M. Calogovic, J. Hasic, D.V. Topic, Inorg. Chim. Acta 285 (1999) 208.
[20] G. Tamasi, S. Defazio, L. Chiasserini, A. Sega, R. Cini, Inorg. Chim. Acta 362 (2009) 1011;
M.D. Gutierrez, R. Lopez, M.A. Romero, J.M. Salas, Canada J. Chem. 66 (1988) 249.
[21] E.L. Torres, M.A. Mendiola, Polyhedron 24 (2005) 1435.
[22] G. Glolub, H. Cohen, P. Paoletti, A. Bencini, D. Meyerstein, J. Chem. Soc., Dalton Trans. 10 (1996) 2055.
[23] I. Gabr, H. El-Asmy, M. Emmam, S.I. Mostafa, Transition Met. Chem. 34 (2009) 409.
[24] M. Guta, M.N. Srivastava, Synth. React. Inorg. Met. Organ., Nano-Met. Chem. 26 (1996) 305.
[25] C.L. Ma, Y. Shi, Q.F. Zhang, Q. Jiang, Polyhedron 24 (2005) 1109.

[26] Z. Popovic, G. Pavlovic, D.M. Calogovic, Z. Soldin, M. Rajic, D.V. Topic, D. Kovacek, Inorg. Chim. Acta 306 (2000) 142.
[27] S.I. Mostafa, S. Abd El-Maksoud, Monatsh. Chem. 129 (1998) 455.
[28] A.G.deA. Fernandes, V.M. Deflon, E.J. de Souza, P.I.S. Maia, A.A. Batista, S.S. Lemos, U. Abram, J. Ellena, E.E. Castellano, Polyhedron 27 (2008) 2983.
[29] A.K. Boudalis, V. Nastopoulos, S.P. Perlepes, C.P. Raptopoulou, A. Terzis, Transition Met. Chem. 26 (2001) 276.
[30] S. Aruna, G. Shanmugam, Spectrochim. Acta 41A (1985) 531.
[31] S.I. Mostafa, K.M. Ibrahim, Z.A. Younis, Inorg. Chem. Ind. J. 2 (2007) 68.
[32] P.K. Santra, C. Sinha, W.J. Sheen, F.L. Liao, T.H. Lu, Polyhedron 20 (2001) 599.
[33] S.I. Mostafa, Transition Met. Chem. 32 (2007) 769.
[34] S.A. Elsayed, A.M. El-Hendawy, S.I. Mostafa, B.J. Jean-Claude, M. Todorova, Ian S. Butler, Bioinorg. Chem. Appl., 2010, doi:10.1155/2010/149149(1-11).
[35] A.R. Johnson, B. O'Sullivan, K.N. Raymond, Inorg. Chem. 39 (2000) 2652.
[36] S.I. Mostafa, M.M. Bekheit, Chem. Pharm. Bull. 48 (2000) 266.
[37] Z. Zhang, S.J. Rettig, C. Orvig, Inorg. Chem. 30 (1991) 509.
[38] A.M. Ouf, M.S. Ali, E.M. Saad, S.I. Mostafa, J. Mol. Struct. 973 (2010) 69.
[39] N.A. Anaan, E.M. Saad, S.M. Hassan, I.S. Butler, S.I. Mostafa, Carbohyd. Res. 346 (2011) 775.
[40] M. Coluccia, A. Nassi, F. Loseto, J. Med. Chem. 36 (1993) 510.
[41] F.P.T. Harmers, W.H. Gispen, J.P. Neijt, Eur. J. Cancer 27 (1991) 372.
[42] S.I. Mostafa, J. Coord. Chem. 61 (2008) 1553.
[43] S.K. Hadjikakou, M.A. Demertzis, M. Kubicki, Appl. Organomet. Chem. 14 (2000) 727.
[44] N.J. Wheate, R.I. Teleb, A.M. Krause-Heuer, R.L. Cook, S. Wang, V.J. Higgins, J.R. Aldrich-Wright, J. Chem. Soc., Dalton Trans. (2007) 5055.
[45] S. Kemp, N.J. Wheate, D.P. Buck, M. Nikac, J.G. Collins, J.R. Aldrich-Wright, J. Inorg. Biochem. 101 (2007) 1049.
[46] A.B. Lansdown, J. Wound Care 11 (2002) 125.
[47] A.B. Lansdown, J. Wound Care 11 (2002) 173.
[48] S.I. Mostafa, I.S. Butler, F. Ibrahim, Y. El-Hawary, CSC2011, Montreal, 2011.